The driving mechanism of roAp stars

2008 J. Phys.: Conf. Ser. 118 012052

(http://iopscience.iop.org/1742-6596/118/1/012052)

Proceedings of the Second HELAS International Conference IOP Publishing
Journal of Physics: Conference Series **118** (2008) 012052 doi:10.1088/1742-6596/118/1/012052

The driving mechanism of roAp stars

M-A Dupret[1], S Théado[2] and A Noels[2]

[1] Observatoire de Paris, LESIA, CNRS UMR 8109, 5 place J. Janssen, 92195 Meudon, France
[2] Institut d'Astrophysique et Géophysique, Université de Liège, Belgium

E-mail: MA.dupret@obspm.fr

Abstract. We analyse in detail the driving mechanism of roAp stars and present the theoretical instability strip predicted by our models with solar metallicity. A particular attention is given to the interpretation of the role played by the different eigenfunctions in the stabilization of the modes at the red edge of the instability strip. The gradient of temperature in the H_I opacity bump appears to play a major role in this context. We also consider the particular and complex role played by the shape of the eigenfunctions (location of the nodes, ...).

1. Introduction

roAp stars are a much studied class of stars with rapid oscillations (4 to 21 minutes), strong magnetic fields (hundreds to a few thousand Gauss) and chemical pecularities with non-uniform distribution both horizontally and vertically. Up to now, 35 roAp stars have been detected. Their rapid oscillations are interpreted as high-overtone, low degree, non-radial p-modes. They mostly lie within the main sequence part of the instability strip as the δ Scuti stars. The driving mechanism of their oscillation modes is still a matter of debate but the most probable explanation seems to be the κ-mechanism acting in the H_I ionisation zone. Many physical processes could play a role in this context: e.g. the coupling with magnetic field [11], the ability of the latter to freeze convection and allow the stratification of chemicals, the role of winds [13].

2. Theoretical instability strips

We have computed stellar models adequate for A stars using the stellar evolution code Clés (described in Scuflaire et al. 2007). The metal mixture used in the computations is the solar one determined by [1] (AGS05) with initial mass fractions of hydrogen and metals respectively equal to X=0.7103 and Z=0.0117. The opacity tables (also computed with the AGS05 mixture) are those of OPAL96 [7] completed at low temperature with tables based upon calculations from [6]. As outer boundary conditions, Kurucz atmospheres [9] are joined to the interior at an optical depth equal to 1. Following works by [2] and [13], we computed models with fully radiative envelope, assuming that the convection is suppressed by the magnetic field. The stability of these models has been computed using the non-adiabatic pulsation code MAD ([4]). Fig. 1 shows the evolution tracks of our models and the deduced theoretical instability strip of roAp stars. Although the agreement is good down to a luminosity of about $\log(L/L_\odot) = 0.9$, our models fail to reproduce the position of the red edge of the instability strip. This is not a surprise since up to now no evolutionary computation was able to account for the excitation of roAp modes in stars with effective temperature lower than 7400 K. All computed models with standard homogeneous composition ([3], [2]) or with stratified distribution induced by He

settling and stellar wind ([13], [14]) failed to shift the red limits towards cooler temperatures. The aim of this poster is then to try to better understand the driving mechanism of roAp stars and to find the reason why high order p-modes are not found to be excited in theoretical models of cool magnetic Ap stars.

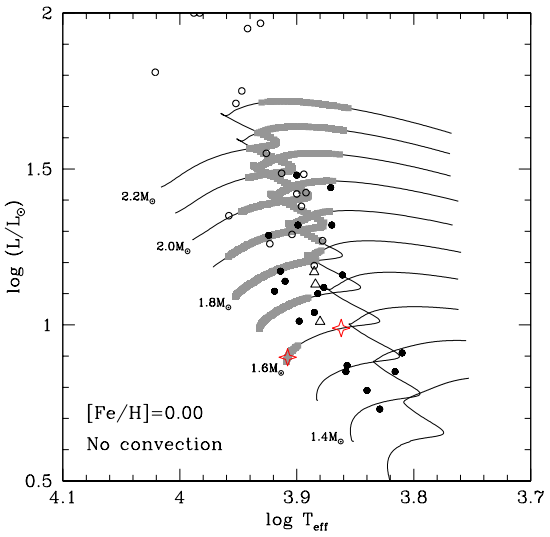

Figure 1. Evolutionary tracks of our models. The gray squares represent the models for which roAp-type modes are found to be excited. The symbols are observational points according to [8] and [10]: solid circles represent roAp stars, open circles are noAp stars and the triangles are roAp candidates.

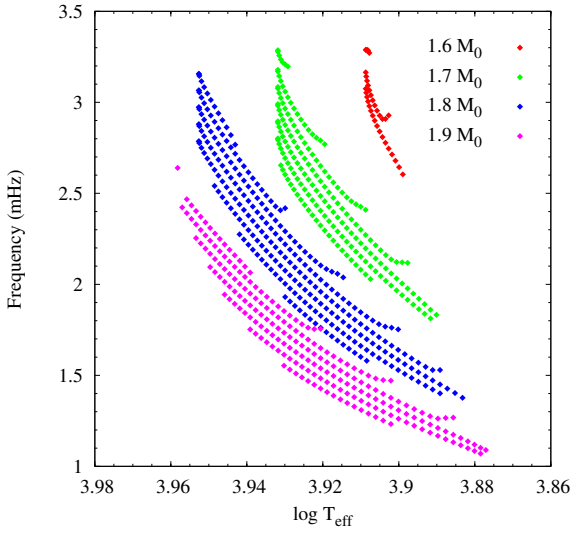

Figure 2. Frequencies (mHz) of the unstable modes predicted by our models as a function of $\log T_{\rm eff}$. The different colors correspond to different masses from 1.6 $M_\odot$ (red) to 1.9 $M_\odot$ (magenta). The main changes come from the different dynamical times: $\tau_{\rm dyn} = (R^3/GM)^{1/2}$ of the models.

3. Driving mechanism of roAp stars

In the present study we neglect the coupling of oscillations with the magnetic field; for the radiative transfer we use the diffusion approximation below the photosphere and we follow the treatment of the thermal aspects proposed by [4] in the atmosphere. In this simplified framework, it is easier to identify and interpret the main features of the driving mechanism in roAp stars. To help the discussion we recall some basic equations for the thermal aspects of stellar oscillations. The perturbed equations of energy conservation and diffusion are, for a radial mode:

$$i\,\sigma\,T\,\delta s \;=\; -\,\frac{{\rm d}\delta L}{{\rm d}m} \quad , \qquad \frac{\delta L}{L} \;=\; 4\,\frac{\delta r}{r} \;+\; 4\,\frac{\delta T}{T} \;-\; \frac{\delta\kappa}{\kappa} \;+\; \frac{{\rm d}(\delta T/T)}{{\rm d}\ln T}\,. \tag{1}$$

The work integral expression giving the mode growth-rate is:

$$\begin{aligned} W(m) \;&=\; -\int_0^m \Im\left\{\frac{\delta\rho^*}{\rho}\frac{\delta P}{\rho}\right\}{\rm d}m \;=\; -\int_0^m (\Gamma_3-1)\Im\left\{\frac{\delta\rho^*}{\rho}T\delta s\right\}{\rm d}m \\ &=\; \int_0^m \nabla_{\rm ad}\,\Im\left\{T\delta s^*\frac{\delta P}{P}\right\}{\rm d}m\,. \end{aligned} \tag{2}$$

In the classical κ-mechanism, the driving of the modes comes from the accumulation of heat during the contraction phase ($\partial\delta L/\partial m < 0$) associated with the changes of $\delta\kappa/\kappa$ (Eq. 1) around opacity bumps. The mechanism is slightly different in roAp stars.

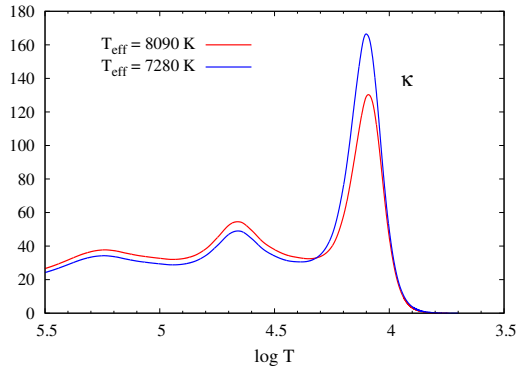

Figure 3. Opacities (cm^2/g) for two compared 1.6 $\mathrm{M}_\odot$ models with different $T_{\rm eff}$.

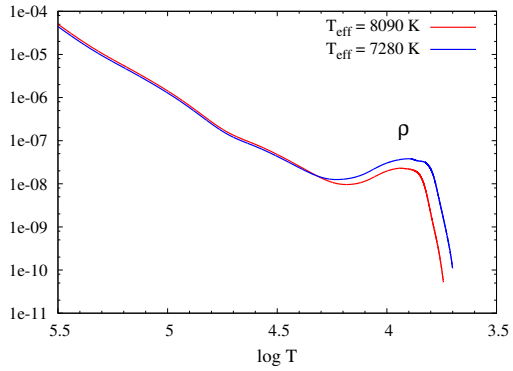

Figure 4. Densities (g/cm^3) for two compared 1.6 $\mathrm{M}_\odot$ models with different $T_{\rm eff}$.

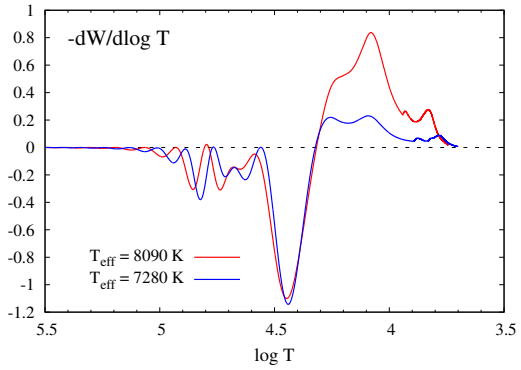

Figure 5. Differential work $-\mathrm{d}W/\mathrm{d}\log T$ for the radial mode p_{32} for two compared 1.6 $\mathrm{M}_\odot$ models with different $T_{\rm eff}$.

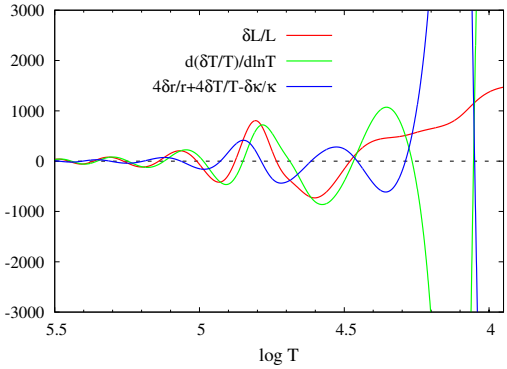

Figure 6. Contributions to $\delta L/L$ for the radial mode p_{32} (see details in the text), model with $T_{\rm eff} = 8090$ K.

Fig. 3 gives the opacities for two 1.6 $\mathrm{M}_\odot$, Z=0.0117 models inside (red) and out (blue) of the instability strip; they are located by red stars in Fig. 1. We compare in detail the results for these two models in this paper. Fig. 4 shows the density distribution for these two models. Note the density inversions resulting from the large opacity bumps. Fig. 5 gives the differential work $-\mathrm{d}W/\mathrm{d}\log T$ for the radial mode p_{32} ($\nu = 3$ mHz for the hot model and $\nu = 1.8$ mHz for the cold model). Positive (resp. negative) regions have a driving (resp. damping) effect on the oscillations. Damping occurs between $\log T = 5$ and $\log T = 4.3$ and driving occurs around the $\log T \simeq 4.1$ opacity bump.

We give in Fig. 6 the contribution of the different terms of Eq. 1. The term $\mathrm{d}(\delta T/T)/\mathrm{d}\ln T$ is given by the green line, the added other contributions to $\delta L/L$ are shown by the blue line and the red line gives the sum. This shows two very different regions. From the center to $\log T \simeq 4.5$, the term $\mathrm{d}(\delta T/T)/\mathrm{d}\ln T$ dominates because the eigenfunctions have many nodes there. Substituting this dominating term in Eq. 2 shows the well known radiative damping mechanism occurring in regions of short-wavelength oscillations. We note that this radiative damping depends on the equilibrium temperature gradient, but not significantly on the fluctuations of the opacity. We consider now the region between $\log T \simeq 4.25$ and the photosphere. Because of the strong opacity bump, $\delta T/T$ explodes in this region (see Fig. 7). This is easily understood: in this region of very small heat capacity, the temperature gradient variations must compensate the opacity

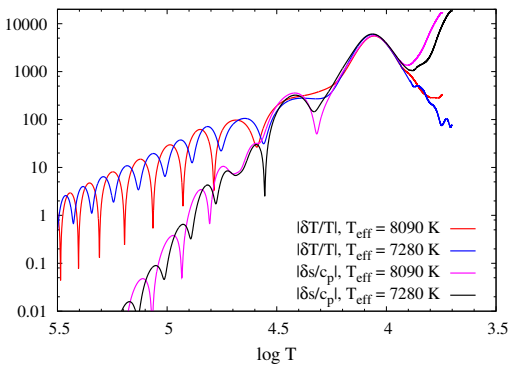

Figure 7. $|\delta T/T|$ and $|\delta s/c_p|$ for two compared 1.6 $M_\odot$ models with different $T_{\rm eff}$.

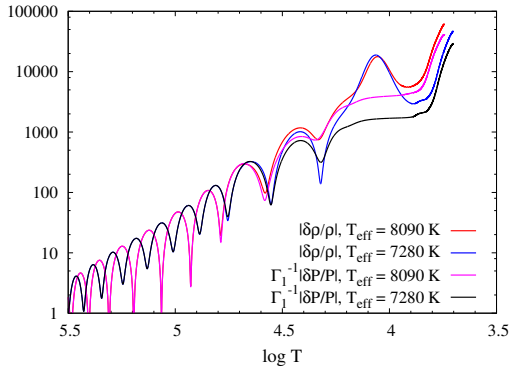

Figure 8. $|\delta\rho/\rho|$ and $\Gamma_1^{-1}|\delta P/P|$ for two compared 1.6 $M_\odot$ models with different $T_{\rm eff}$.

variations to ensure the energy balance (small $|\partial\delta L/\partial r|$). Hence $\delta T/T$ follows more or less the shape of the temperature gradient.

Because the pressure is controled by the movement equation $\mathrm{d}\delta P/\mathrm{d}r = g\rho(4+\sigma^2 r/g)\,\delta r/r$, it cannot follow the huge temperature variations. Having $|\delta P/P| << |\delta T/T|$, we get from the perturbed equation of state: $\delta s/c_p \approx \delta T/T \approx -\delta\rho/\rho$ in the H_I opacity bump (see Fig. 7). The heat exchanges are thus very large and much energy can be given or taken from the modes. The result as a driving or damping depends on the respective phases of the eigenfunctions. There, $\delta\rho/\rho$ is more or less in opposite phase with $\delta s/c_p$ and $\delta T/T$, so it does not help to know if we have driving or damping. It is better to consider the phase differences with respect to δP. From Eq. 2, we see that heat must be received ($\mathrm{d}\delta Q/\mathrm{d}t > 0$) when $\delta P > 0$ to have a driving of the modes ($0° < \phi(\delta P) - \phi(\delta s) < 180°$). This appears to be the case for the radial mode p_{32} considered here and it is thus excited. But for other modes whose last node location is not the same with respect to the H_I opacity bump the contrary can occurs and they are damped. This will be discussed with more details in Sect. 5.

The driving mechanism of roAp stars is thus not exactly the same as the classical κ-mechanism. In the latter case, the fact that $\partial \ln\kappa/\partial \ln P|_s$ and thus $|\delta\kappa/\kappa|$ increase outwards automatically implies that $\mathrm{d}\delta L/\mathrm{d}m < 0$, so heat is gained during contraction and transformed in mechanical work. In the H_I opacity bump of roAp stars, the opacity variations are counterbalanced by the temperature gradient variations and the total result as a positive or negative heat exchange and mechanical work depends on the modes.

4. What determines the red edge of the roAps instability strip ?

The physical processes determining the instability strip red edge are very different in our roAp models compared to other κ-driven oscillators such as δ Sct stars. In the latter case, the damping of the modes comes from the time-dependent coherent coupling with convection ([5]). In our purely radiative roAp models we predict also a red edge, so we must search for another explanation.

As can be seen in Fig. 3, the H_I opacity bump of cold models out of the instability strip is larger than inside the instability strip. The very high temperature gradient in this region implies a density inversion which is stronger for the cold model (Fig. 4). *With this in mind, we could have expected more driving in the cold model compared to the hot one (at least in a classical κ-mechanism vision of the problem) but the contrary occurs.* We also note that the radiative damping is more or less the same in the two models (see Fig. 5), because the temperature gradient and the eigenfunctions are very similar in this region for different models. The explanation of

the red edge comes from a closer study of the eigenfunctions and their respective phases in the H_I opacity bump.

As already explained above and shown in Fig. 7 and 8, $|\delta s/c_p| \simeq |\delta T/T| \approx |\delta\rho/\rho| >> |\delta P/P|$ in the H_I opacity bump region. We note also in these figures that the values obtained for $|\delta s/c_p|$ in this region are very close for the hot and cold models. But the values of $|\delta P/P|$ are much smaller in the cold model compared to the hot one. As told before, to see how much driving occurs in this region, it is here better to consider the work expression in term of δP instead of $\delta\rho$. As $|\delta P/P|$ is much smaller in the cold model, $|\Im(T\delta s^*\delta P/P)|$ is smaller and less work is performed (see Eq. 2). This smaller driving cannot counterbalance the radiative damping of the deeper layers and all modes are stable.

So, as this is the key, we just have to understand now why $|\delta P/P|$ is much smaller in the cold model compared to the hot one in this region. In the asymptotic adiabatic regime, the scale height of variation of the eigenfunctions is given by c/σ which remains valid here for $\delta P/P$ (c is the sound speed and σ the angular frequency). But the scale height of variation of the other thermodynamic eigenfunctions is $-\mathrm{d}r/\mathrm{d}\ln T$ as they are shaped by the opacity bump. This gives a ratio: $[c/(\omega\sqrt{GM}][R^{3/2}\mathrm{d}\ln T/\mathrm{d}r]$ which is larger for the cold model than for the hot one, because of its larger temperature gradient (the first bracket where appear the dimensionless frequency ω and c ($\propto T$) is more or less the same in the two models). Hence $\delta P/P$ cannot reach high enough values around the H_I opacity bump of the cold model and its high order p-modes are stable.

5. Shape and nodes of the eigenfunctions

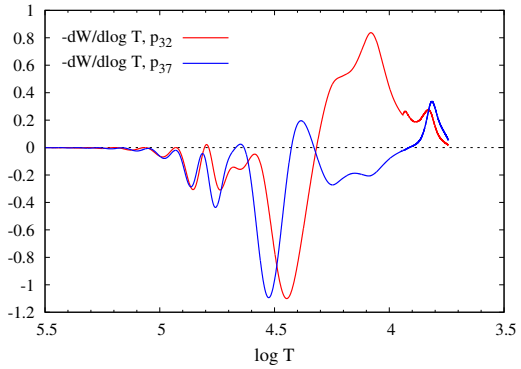

Figure 9. Comparison of the differential work $-\mathrm{d}W/\mathrm{d}\log T$ for the radial modes p_{32} and p_{37}, 1.6 $M_\odot$ model with $T_{\rm eff} = 8090$ K.

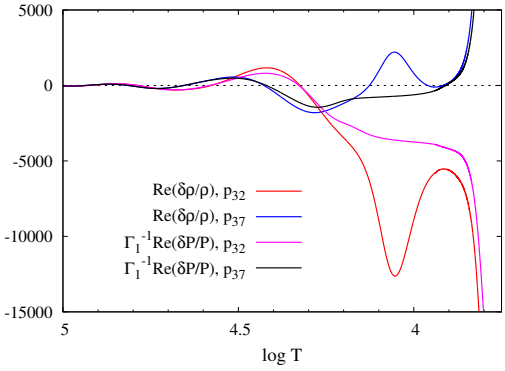

Figure 10. $\Re\{\delta\rho/\rho\}$ and $\Gamma_1^{-1}\Re\{\delta P/P\}$ for the radial modes p_{32} and p_{37}, 1.6 $M_\odot$ model with $T_{\rm eff} = 8090$ K.

It is important to emphasize that the predictions concerning the driving and damping mechanisms in roAp stars are extremely sensitive to the shape of the eigenfunctions. For these very high radial order p-modes, nodes can appear in the driving region and in the atmosphere. The latter phenomenon is not purely theoretical, it is observed in the line-profile variations of some roAp stars. As an example, we compare in Figs. 9 and 10 the results obtained for the same hot model as before, but for two different modes: p_{32} and p_{37}. We see in fig. 9 where $-\mathrm{d}W/\mathrm{d}\log T$ is given that the mode p_{37} is damped almost everywhere ! To understand this, we compare in Fig. 10 $\Re(\delta\rho/\rho)$ and $\Gamma_1^{-1}\Re(\delta P/P)$. For p_{37}, $\delta\rho/\rho$ has a node at $\log T \approx 4.1$ but not $\delta P/P$, which changes the sign of $\Im(\delta\rho^*\delta P)$. Hence, instead of having driving, we have damping in the H_I opacity bump (see Eq. 2). The location of the nodes makes a kind of windowing in the driving mechanism of roAp stars. They must be just at the right place, out of the H_I opacity

bump. This windowing explains why the theoretical frequency interval of unstable modes is small for any given roAp model (Fig. 2).

6. Conclusions

Our analysis of the driving mechanism of roAp stars shows that radiative damping dominates in a region where their high order pressure mode eigenfunctions have many nodes (between $\log T = 5.1$ and $\log T = 4.3$). This damping is counterbalanced by a significant driving occurring in the H_I opacity bump ($\log T \simeq 4.1$). The stabilization of the modes at the red side of the instability strip is due to the temperature gradient which becomes too large in this region for the cold models. As a consequence, $|\delta P/P|$ is smaller in the cold model, which inhibits the driving effect of the H_I opacity bump. The location of the nodes of the eigenfunctions in the very superficial layers is important, they must be out of the opacity bump to allow enough driving. *The nodes location make a kind of windowing in the driving mechanism of roAp stars, restricting the frequency interval of unstable modes.*

References

[1] Asplund M, Grevesse, N and Sauval A J 2005 *ASPC* **336** 25
[2] Balmforth N J, Cunha M S, et al. 2001 *MNRAS* **323** 362
[3] Cunha M S 2002 *MNRAS* **333** 47
[4] Dupret M A, De Ridder J, et al. 2002 *A&A* **385** 563
[5] Dupret M A, Grigahcène A, Garrido R, et al. 2005 *A&A* **435** 927
[6] Ferguson J W, Alexander D R, et al. 2005 *ApJ* **623** 585
[7] Iglesias C A and Rogers F J 1996 *ApJ* **464** 943
[8] Kochukhov O and Bagnulo S, 2006, *A&A* **450** 763
[9] Kurucz R L, 1998, http://kurucz.harvard.edu/grids.html
[10] North P, Jaschek C, et al. 1997 *ESA SP-402* 239-244
[11] Saio H 2005 *MNRAS* **360** 1022
[12] Scuflaire R, Théado S, et al. 2007 *ApSS* in press
[13] Théado S, Vauclair S, Cunha M S 2005 it A&A **443** 627
[14] Théado S, Cunha M S 2006 *CoAst* **147** 101